Received: 16 October 2018 | Revised: 10 March 2019 | Accepted: 17 April 2019

DOI: 10.1002/hipo.23098

RESEARCH ARTICLE

WILEY

Postnatal nectin-3 knockdown induces structural abnormalities of hippocampal principal neurons and memory deficits in adult mice

Rui Liu[1] | Han Wang[1] | Hong-Li Wang[1] | Ya-Xin Sun[1] | Yun-Ai Su[1] | Xiao-Dong Wang[2] | Ji-Tao Li[1] | Tian-Mei Si[1]

[1]National Clinical Research Center for Mental Disorders (Peking University Sixth Hospital/Institute of Mental Health) and the Key Laboratory of Mental Health, Ministry of Health (Peking University), Beijing, China

[2]Department of Neurobiology, Key Laboratory of Medical Neurobiology of Ministry of Health of China, Zhejiang Province Key Laboratory of Neurobiology, Zhejiang University School of Medicine, Hangzhou, China

Correspondence
Tian-Mei Si and Ji-Tao Li, National Clinical Research Center for Mental Disorders (Peking University Sixth Hospital/Institute of Mental Health) and the Key Laboratory of Mental Health, Ministry of Health (Peking University), Beijing 100191, China.
Emails: si.tian-mei@163.com and ljt_102124@163.com

Funding information
Beijing Brain Project, Grant/Award Number: Z171100000117016; National Key Basic Research Program of China, Grant/Award Number: 2015CB856401; Peking University Medicine Seed Fund for Interdisciplinary Research, Grant/Award Number: BMU2017MX021; National Natural Science Foundation of China, Grant/Award Numbers: 81571312, 81571321, 81630031

Abstract

The early postnatal stage is a critical period of hippocampal neurodevelopment and also a period of high vulnerability to adverse life experiences. Recent evidence suggests that nectin-3, a cell adhesion molecule, mediates memory dysfunction and dendritic alterations in the adult hippocampus induced by postnatal stress. But it is unknown whether postnatal nectin-3 reduction alone is sufficient to alter hippocampal structure and function in adulthood. Here, we down regulated hippocampal expression of nectin-3 and its heterophilic adhesion partner nectin-1, respectively, from early postnatal stage by injecting adeno-associated virus (AAV) into the cerebral lateral ventricles of neonatal mice (postnatal day 2). We found that suppression of nectin-3, but not nectin-1, expression from the early postnatal stage impaired hippocampus-dependent novel object recognition and spatial object recognition in adult mice. Moreover, AAV-mediated nectin-3 knockdown significantly reduced dendritic complexity and spine density of pyramidal neurons throughout the hippocampus, whereas nectin-1 knockdown only induced the loss of stubby spines in CA3. Our data provide direct evidence that nectins, especially nectin-3, are necessary for postnatal hippocampal development of memory functions and structural integrity.

KEYWORDS
hippocampus, memory, morphology, nectin-3, neurodevelopment

1 | INTRODUCTION

Dendritic structural plasticity strongly influences local signal integration and molecular interaction that are essential for precise brain circuit functions and behaviors (Alvarez & Sabatini, 2007; Lupien, McEwen, Gunnar, & Heim, 2009; Yuste, 2011). Aberrant dendritic arbors and spines have been implicated to involve in many neuropsychiatric disorders, including schizophrenia, bipolar disorder, and Alzheimer's disease (Bhatt, Zhang, & Gan, 2009; Forrest, Parnell, & Penzes, 2018).

The early postnatal stage is a critical period of neurodevelopment. Experience-dependent activities in early life can interact with genetic imprinting to shape neural dendritic plasticity and influence brain structure and function (Lupien et al., 2009). Hippocampal principal cells are extraordinarily vulnerable to the disruption of early-life neurodevelopment, such as by exposure to stressful life

The data that support the findings of this study are available from the corresponding author upon reasonable request.

events (Liao et al., 2014). Accumulating evidence indicates that early-life stress leads to abnormal growth of dendrites and spines in hippocampus, as well as dramatic and enduring deficits of hippocampus-dependent learning and memory, which may contribute to stress-related neuropsychiatric disorders (Liao et al., 2014; Liu et al., 2016; Turecki, Ota, Belangero, Jackowski, & Kaufman, 2014; Wang et al., 2013). Understanding the molecular mechanisms of early-life hippocampal neurodevelopment may provide insight into the pathophysiology of stress-related mental illness.

Synaptic cell adhesion molecules (CAMs) are trans-synaptic anchors and mediators of experience-dependent signaling and dynamically modulate synaptic activity and plasticity (Dalva, McClelland, & Kayser, 2007; Shapiro, Love, & Colman, 2007). They participate in early synaptogenesis, neural growth, synaptic maturation, and remold synaptic function through interaction with diverse synaptic proteins and receptors (Dalva et al., 2007; Parrish, Emoto, Kim, & Jan, 2007). CAM dysfunction-induced spine and functional abnormalities have been strongly implicated in several cognition-related neuropsychiatric disorders (Jamain et al., 2003; Kirov et al., 2008; Sandi, 2004; Yan et al., 2005). Among them, nectin-3 is a Ca^{2+}-independent, Ig-like CAM that is abundant in neonatal and adult hippocampal pyramidal neurons and plays key roles in hippocampus-dependent cognitive functions (Mizoguchi et al., 2002; Takai, Miyoshi, Ikeda, & Ogita, 2008; Wang et al., 2017). Nectin-3 localizes on the postsynaptic membrane, forms the heterophilic adherens junction with its presynaptic partner, nectin-1, and triggers the recruitment of actin cytoskeleton and cadherin–catenin complex for synaptic formation, stabilization, and remolding (Mizoguchi et al., 2002; Tachibana et al., 2000; Togashi et al., 2006).

A growing number of studies suggest that hippocampal nectin-3 is susceptible to various stress challenges, and is implicated in stress-induced aberrant neural structure and cognitive dysfunction (Liao et al., 2014; van der Kooij et al., 2014; Wang et al., 2013, 2017). Recently, we reported that early-life stress resulted in persistent suppression of nectin-3 expression in hippocampus from postnatal stage (Liao et al., 2014; Wang et al., 2013). Although some studies have explored the function of nectin-3 in hippocampus using transgenic technology or virus injection to knock down hippocampal nectin-3 level in embryonic period or adulthood (Honda et al., 2006; Miyata et al., 2017; Wang et al., 2013), none of these studies have examined whether postnatal nectin-3 knockdown could reproduce negative stress effects on hippocampus.

In the current study, we aim to directly examine the involvement of nectins in postnatal hippocampal development by investigating the influences of hippocampal nectin-3 and nectin-1 knockdown on hippocampus-dependent memory and dendritic complexity and spine density in hippocampal principal neurons. The knockdown was carried out by intracranial injection of adeno-associated virus (AAV) into the cerebral lateral ventricles of neonatal mice (Kim et al., 2013) at postnatal day 2 (P2), the beginning time point of the early-life stress procedure we adopted (Liao et al., 2014; Wang et al., 2013). Our findings highlight an important role for nectin-3, but not nectin-1, in postnatal hippocampal development.

2 | MATERIALS AND METHODS

2.1 | Animals and housing

Adult male and female C57BL/6N mice (12-week-old; Vital River Laboratories, Beijing, China) were used for breeding. After arrival, mice were single housed and habituated in the vivarium for 2-week habituation. After habituation, each female was housed with one male for 2 weeks and then single-housed. Pregnant females were monitored daily at 10:00 and 15:00 to keep accurate records of pup delivery time. The day of pup delivery was defined as P0. Considering that estrogen is a potent modulator for structural plasticity (Griffin & Flanagan-Cato, 2008; Spruston, 2008), only male offspring were used in the experiments.

All mice were housed under a standard condition (12-hr light/dark cycle, lights on 08:00–20:00 hr, temperature 23 ± 1°C, 35–55% relative humidity) with free access to food and water. The male pups were randomly assigned to each group at P2. All procedures were approved by the Peking University Committee on Animal Care and in accordance with the National Institute of Health's Guide for the Use and Care of Laboratory Animals.

2.2 | Experimental procedure

On the morning of P2, pups were weighed and given an intracranial AAV injection. Before injection, the home cage containing the litter was placed on a heating pad maintained at 30–35°C. The dam was then removed from the litter and transferred to a clean cage. Each litter was randomly assigned to the groups of nectin-3 knockdown (N3_KD), nectin-1 knockdown (N1_KD), and controls (CT). The duration of injection was limited to ≤20 min per litter. After injection, the dam was placed back to the home cage for normal breeding. Male offspring were weaned on P28 and group-housed in 4 per cage. Mice were subjected to a series of behavioral tests from P75 and were killed 24 hr after behavioral testing for molecular analysis. Another cohort was directly killed at P75 for morphological analysis. A new cohort of N3_KD and control male offspring were killed at P16 for molecular and morphological analyses to test whether the observed CA3 structural abnormalities at P75 induced by nectin-3 knockdown occurred in the early postnatal period. For all experiments, pups included in each group were obtained from 3–5 litters.

2.3 | Viral microinjection

We used AAV8 vectors prepared by Obio Technology (Shanghai, China) to suppress nectin-3 and nectin-1 expression. The short hairpin (sh) RNA sequences targeting *nectin-3* and *nectin-1* were 5′-TGTGTCCTGGA GGCGGCAAAGCACAACTT-3′ and 5′-GCAGCTATGAGGAGGAAGA

GG-3′, respectively. AAV-shNectin-3 (AAV8-CMV-bGlobin-eGFP-H1-shNectin3, 3.9×10^{12} viral genomes/mL), AAV-shNectin-1 (AAV8-CMV-bGlobin-eGFP-H1-shNectin1, 1.0×10^{12} viral genomes/mL) and the control virus (AAV8-CMV-bGlobin-eGFP-H1-shScrambled, 3.5×10^{12} viral genomes/mL) were used. All the viral vectors were packaged and affinity purified (GeneDetect).

Neonatal mice (P2) were anesthetized with isoflurane before injection. Following cessation of movement, bilateral viral microinjections (0.5 μL/hemisphere) were performed using a 1 μL Hamilton syringe (Hamilton, 7001) with a 33 gauge needles (Hamilton, 65461–01). The injection site was located approximately 1 mm lateral to the sagittal suture, halfway between the lambda and bregma, which targeted the lateral ventricles to ensure virus transduction into hippocampus (Gholizadeh, Tharmalingam, Macaldaz, & Hampson, 2013; Kim et al., 2013). The needle was held perpendicular to the skull surface during insertion to a depth of approximately 3 mm. Once the needle was in place, 0.5 μL of viral solution was manually injected into each lateral ventricle. The micropipette was left in the site for additional 2 min to avoid backstreaming.

2.4 | Behavioral testing

Behavioral tests were performed between 09:00 and 15:00 as previously described (Li et al., 2017). The open field test was automatically scored by ANY-maze 4.98 (Stoelting, Wood Dale, IL). Other behavioral tests were scored by an investigator blind to treatment conditions.

2.4.1 | Open field test

Mice were placed in the open field arena ($50 \times 50 \times 50$ cm^3) made of gray polyvinyl chloride and evenly illuminated at 60 lx. During the test, mice were allowed to freely explore the apparatus for 10 min. The time in the center zone (20×20 cm^2), the latency to the center zone, and total distance traveled were analyzed.

2.4.2 | Novel object recognition task

The test protocol was adapted from previous work (Ozawa et al., 2006). During the test, the open field arena was under low illumination (10 lx) and no spatial cue was provided. Before the testing day, mice were habituated to the testing environment for 10 min on two trials (with 60 min interval). The testing procedure consisted of two consecutive trials separated by 60 min. In the training trial, mice were presented with two identical object A (circular cones), and allowed to explore for 10 min. In the retrieval trial, one of the familiar objects used during training was replaced by a novel object B (pyramid), and the mice were allowed to explore freely for 10 min. The time spent exploring each object was recorded. The discrimination index (DI) was calculated as: 100% × time with the novel object/time with both objects.

2.4.3 | Spatial object recognition task

The test was performed in the open field arena under low illumination (10 lx). Prominent spatial cues were provided. Before the testing day, mice were habituated to the testing environment for 10 min on two trials (with 60 min interval). The testing procedure consisted of two consecutive trials separated by 60 min. During the training trial, two identical objects C (cubes) were placed into the open field, and mice were allowed to explore freely for 10 min. In the retrieval trial, mice were presented with a nondisplaced (stationary) object C and a relocated (displaced) one. The time spent exploring each object was measured. The DI was calculated as: DI = 100% × time with the displaced object/time with both objects.

2.4.4 | Y-maze spontaneous alternation task

The Y-maze apparatus was made of gray polyvinyl chloride with three symmetrical arms ($30 \times 10 \times 15$ cm^3) and illuminated at 10 lx. Prominent extramaze spatial cues were provided. Mice were placed in the center zone of arms and allowed to freely explore the maze for 5 min. The number of arm entries, spontaneous alternation ratio, alternate arm return ratio, and same arm return ratio were scored.

2.5 | Immunostaining and image analysis

Mice were anesthetized with sodium pentobarbital (200 mg/kg, intraperitoneally) and transcardially perfused with 0.9% saline followed by 4% buffered paraformaldehyde. Following post fixation and cryoprotection, serial coronal sections were prepared through the dorsal hippocampus (Bregma −1.34 to −2.30 mm) at 30 μm thickness and 180 μm intervals using acryostat (Leica, Wetzlar, Germany). The following primary antibodies were used for immunofluorescence: rabbit anti-nectin-3 (1:1,000; ab63931, Abcam, Cambridge, UK), rabbit anti-nectin-1 (1:1,000; ab66985, Abcam) and rabbit anti-neuronal nuclei antigen (NeuN; 1:5,000, ab104225, Abcam).

For immunofluorescence, sections were treated with 1% normal donkey serum (60 min) and labeled with primary antibodies at 4°C (overnight). The next day, sections were rinsed and labeled with Alexa Fluor 594-conjugated donkey anti-rabbit secondary antibody (1:500; Invitrogen, Carlsbad, CA) for 3 hr at room temperature. After rinsing, sections were transferred onto slides and coverslipped with Vectashield containing 4′,6-diamidino-2-phenylindole (Vector Laboratories, Burlingame, CA).

During image analysis, brain sections were randomly coded so that investigators were blind to the experimental conditions. Images were taken at ×100 using an Olympus IX71 microscope equipped with a charge-coupled device camera (CoolSNAP MP5, Roper Scientific Corporation, Tucson, AZ). Five sample images of both hemispheres for each animal were used for analysis. Optical density values of nectin-1 and nectin-3 were analyzed using NIH ImageJ software. Relative protein levels were determined by the differences in optical density values between the region of interest and the corpus callosum, which generally lacks staining and was set as the background.

The density of NeuN-positive cells was analyzed by ImageJ. Images of NeuN$^+$ neuron immunofluorescence straining ($1{,}024 \times 1{,}024$ pixel^2) were obtained with an Olympus IX81 laser-scanning confocal microscope (Olympus, Tokyo, Japan) at ×20 objective magnification using the Kalman

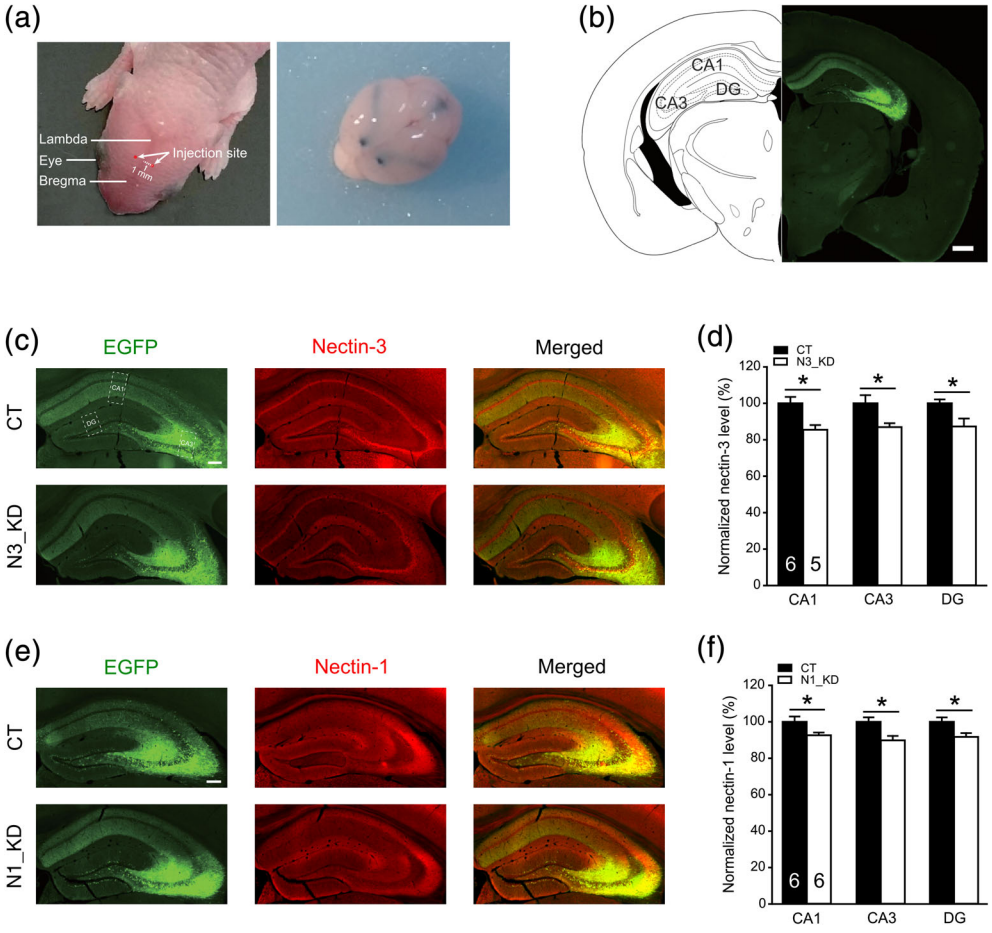

FIGURE 1 Intracranial injection of AAV-shNectin-3/Nectin-1 into the cerebral lateral ventricles of neonatal mice to knock down nectin-3 or nectin-1 levels in the adult dorsal hippocampus. (a) Left: the head of a P2 C57BL/6N mouse showing the target injection sites. Right: schematic showing the effect of intracranial bilateral dye injection into the cerebral lateral ventricles of P2 C57BL/6N mice. (b) Representative images showing the expression of enhanced GFP (EGFP) in adult mouse brain, indicative of hippocampal neurons infected by AAV virus. Scale bars = 1 mm. (c) Images showing EGFP- and/or nectin-3-expressing in the adult dorsal hippocampus. Scale bar = 200 μm. (d) Nectin-3 knockdown significantly reduced nectin-3 levels in the CA1, CA3, and DG of adult hippocampus. (e) Images showing EGFP- and/or nectin-1-expressing in the adult dorsal hippocampus. Scale bar = 200 μm. (f) Nectin-1 knockdown significantly reduced nectin-1 levels in the CA1, CA3, and DG of adult hippocampus. *$p < .05$. AAV, adeno-associated virus; CT, control; DG, dentate gyrus; N1_KD, nectin-1 knockdown; N3_KD, nectin-3 knockdown

filter and sequential scanning mode under identical settings for laser power, photomultiplier gain and offset. Images were adjusted for optimal brightness and contrast using the FV10-ASW 1.7 Software (Olympus). All results were normalized by taking the mean value of the control group as 100%.

2.6 | Golgi-Cox staining and image analysis

Mice were anesthetized with sodium pentobarbital (200 mg/kg, intraperitoneally) and transcardially perfused with 0.9% saline. Brains were dissected and immersed in the Golgi-Cox solution (Glaser & Van der Loos, 1981) for 14 days and then transferred to the 30% sucrose solution for 5 days in the dark at room temperature. In this study, structure changes in CA3 were of our primary interest, because the subregion is abundant with nectin-3, and is highly vulnerable to postnatal stress (Liao et al., 2014; Liu et al., 2016; Mizoguchi et al., 2002; Thompson et al., 2008). To maximize the intactness of apical dendrites of CA3 pyramidal neurons, horizontal sections (200 μm) were prepared using a Microm HM 650 V vibratome (Thermo Scientific, Walldorf, Germany). The free-floating sections were collected on Superfrost plus slides (Thermo Scientific) and processed as described previously (Liao et al., 2014; Wang et al., 2013).

To quantify the dendrite morphology in dorsal hippocampus, 5–8 fully Golgi-impregnated CA3 pyramidal neurons (including 4–6 short-shaft and 1–2 long-shaft neuronal subpopulations (Fitch, Juraska, & Washington, 1989) and dentate gyrus (DG) granule cells (including 3–4 suprapyramidal blades and infrapyramidal blades neurons, respectively) were randomly chosen. The number of analyzed neurons among animals was equal for each group. Neurons were traced at ×400 with the Neurolucida software (MicroBrightField Bioscience, Williston, VT), and Sholl analysis was performed to measure total dendritic length and the number of intersections at concentric circles (20 μm apart) using the NeuroExplorer software (MicroBrightField). Neurons in CA1 were excluded from dendritic analysis, because they were frequently truncated in horizontal sections. To quantify spine density, dendrites (5–8 per animal) located in the stratum radiatum of CA3, CA1, and dendrites (8 per animal) located in the medial molecular layer of DG were digitized at ×1,000 using a CoolSNAP MP5 CCD

camera (Roper Scientific, Tucson, AZ) mounted on an Olympus BX51 microscope. Dendritic spines were identified and categorized as previously described (Liao et al., 2014; Liu et al., 2016; Turecki et al., 2014; Wang et al., 2013).

2.7 | Statistical analysis

SPSS 19.0 (SPSS, Chicago, IL) was used to perform statistical analyses. The discrimination indices of object recognition tasks in each group were compared with 50% using one-sample *t* test to indicate whether animals could distinguish the novel object or location from the familiar one. Comparisons among the three groups (CT, N1_KD, and N3_KD) were carried out using one-way analysis of variance (ANOVA), followed by Tukey's post hoc test when appropriate, and this analysis was applied to behavioral measures in the open field, Y-maze, and object recognition tasks together with dendritic length and spine density in CA3 at P75. The number of dendritic intersections was analyzed by one-way repeated measures ANOVA (with group as the between-subject factor and distance from the soma as the within-subject factor) followed by Bonferroni post hoc test when appropriate. The two-tailed Student's *t* test was used to compare pairs of means. Statistical outliers with values that fell beyond two standard deviations from the mean were excluded from analysis. Data are reported as mean ± *SEM*. Statistical significance was defined at $p < .05$.

3 | RESULTS

3.1 | Neonatal intraventricular virus injection suppressed nectin-3 and nectin-1 expression in adult hippocampus

To knock down nectin-3 and nectin-1 levels in hippocampus at early postnatal stage, we injected AAV-shNectin-3/Nectin-1 into the cerebral ventricles of neonatal mice (Figure 1a,b). We examined nectin-3 and nectin-1 expression levels in the adult dorsal hippocampus and found that nectin-3 immunoreactivity in the CA1, CA3, and DG neurons was significantly reduced in N3_KD mice (CA1: $t_9 = 3.186$, $p = .011$; CA3: $t_9 = 2.467$, $p = .036$; DG: $t_9 = 2.406$, $p = .040$; unpaired *t* test; Figure 1c,d and Figure S1a). Similar reduction of nectin-1 was observed in N1_KD mice (CA1: $t_{10} = 2.252$, $p = .048$; CA3: $t_{10} = 2.948$, $p = .015$; DG: $t_{10} = 2.613$, $p = .026$; unpaired *t* test; Figure 1e,f and Figure S1b). Other brain regions were not analyzed in this study, because the infection was mostly limited in hippocampus (Figure 1b) and we mainly focused on the effects of nectin-3/nectin-1 downregulation on hippocampal structure and hippocampus-dependent memory functions.

3.2 | Postnatal nectin-3, but not nectin-1, knockdown impaired novel and spatial object recognition

In this section, we examined whether reduced nectin-3 or nectin-1 protein expression in the hippocampus from postnatal stage could impair hippocampus-dependent cognitive functions. We observed that neither nectin-3 nor nectin-1 knockdown affected behaviors in the open field (Figure S2a) in terms of total distance traveled ($F_{2,37} = 0.111$, $p = .896$; one-way ANOVA), time spent in the center zone ($F_{2,37} = 0.042$, $p = .959$; one-way ANOVA), and latency to the center zone ($F_{2,37} = 0.005$, $p = .995$; one-way ANOVA). Nevertheless, N3_KD, not N1_KD, mice exhibited significant memory deficits. In the novel object recognition task (Figure 2a), N3_KD mice failed to discriminate the novel object from the familiar one ($t_{13} = 0.370$, $p = .717$; one-sample *t* test), whereas control and N1_KD mice spent significantly more time exploring the novel object than the familiar one (CT: $t_{13} = 9.404$, $p < .001$; N1_KD: $t_{13} = 4.340$, $p = .001$; one-sample *t* test).

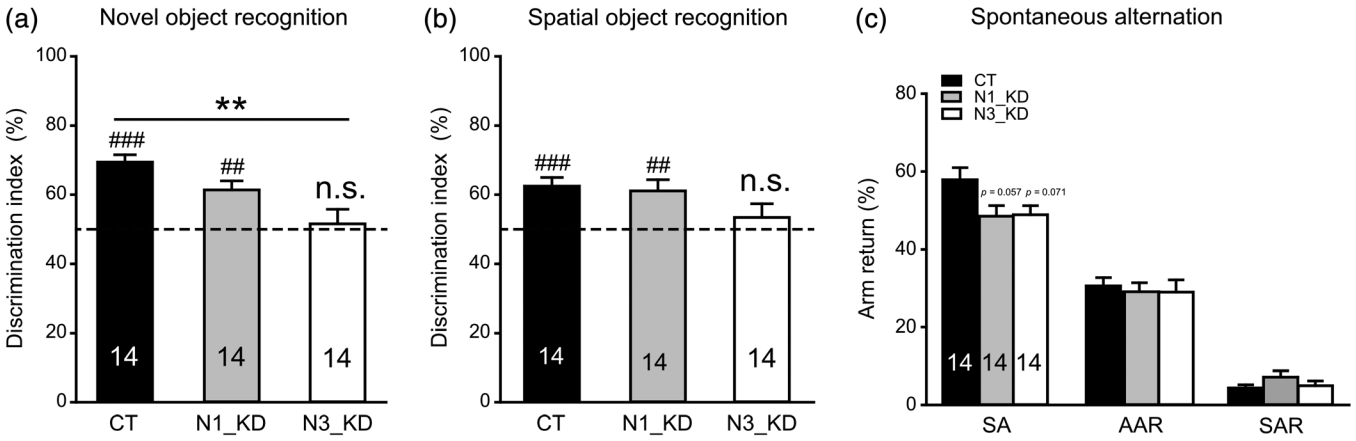

FIGURE 2 Effects of postnatal nectin-3 or nectin-1 knockdown on cognition in adult mice. (a) Mice with postnatal nectin-3 knockdown failed to distinguish the novel object from the familiar one in the novel object recognition task and showed significantly lower discrimination indices than control mice. (b) While control and N1_KD mice distinguished the displaced object from the stationary one in the spatial object recognition task, mice with postnatal nectin-3 knockdown failed to do so. (c) Animals with postnatal nectin-3 or nectin-1 knockdown showed tendency of reduced spontaneous alternation ratios in the Y maze. $^{**}p < .01$, compared with the control group. $^{\#\#}p < .01$, $^{\#\#\#}p < .001$, compared with the chance level (50%), which was denoted by dotted lines. AAR, alternate arm return; CT, control; N1_KD, nectin-1 knockdown; N3_KD, nectin-3 knockdown; n.s., not significant; SA, spontaneous alternation; SAR, same arm return

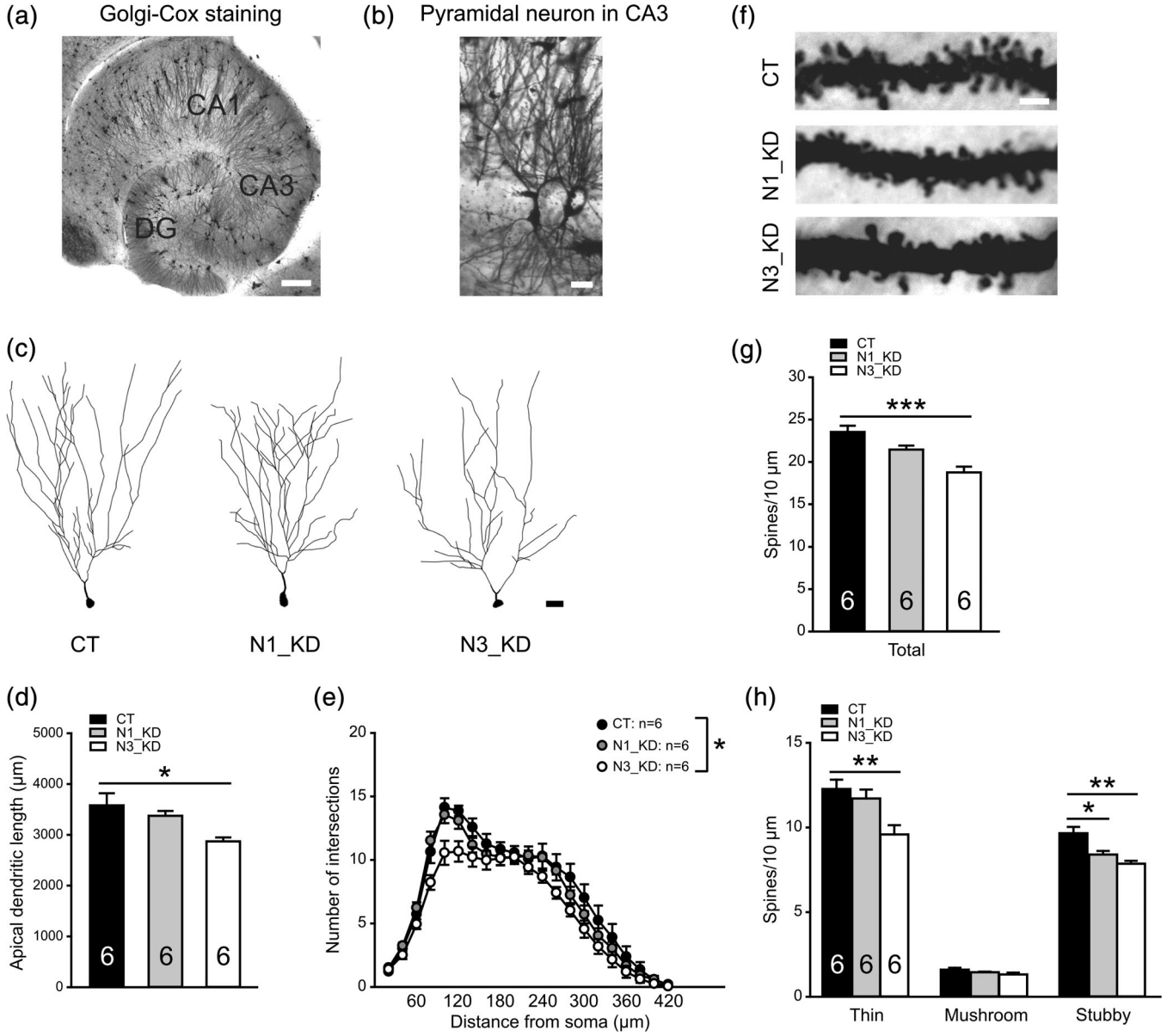

FIGURE 3 Effects of postnatal nectin-3 or nectin-1 knockdown on the morphology of the CA3 pyramidal neurons in adult dorsal hippocampus. (a) A Golgi-stained horizontal section showing the region of hippocampus. Scale bar = 200 μm. (b) Representative photomicrographs of apical dendrites of CA3 pyramidal neurons. Scale bar = 20 μm. (c) Representative tracings of CA3 pyramidal neurons in the three groups. Scale bar = 25 μm. (d–e) Total length and complexity of apical dendrites in three groups, with significant reductions following postnatal nectin-3 knockdown. (f) Photomicrographs of apical dendritic segments of CA3 pyramidal neurons. Scale bar = 2 μm. (g, h) Postnatal nectin-3 knockdown reduced the density of spines, especially the thin and stubby spines, whereas postnatal nectin-1 knockdown only reduced the number of stubby spines. *p < .05, **p < .01, ***p < .001, compared with the control group. CT, control; N1_KD, nectin-1 knockdown; N3_KD, nectin-3 knockdown

Moreover, the discrimination indices of N3_KD mice were significantly lower than those of control mice ($F_{2,39}$ = 8.265, p = .001; one-way ANOVA; CT vs. N1_KD: p = .173; CT vs. N3_KD: p = .001; Tukey's post hoc test). In the spatial object recognition task (Figure 2b), no difference in DI was found among groups ($F_{2,39}$ = 2.138, p = .131; one-way ANOVA), but N3_KD mice failed to show object discrimination (t_{13} = 0.863, p = .404; one-sample t test) as other groups did (control: t_{13} = 4.898, p < .001; N1_KD: t_{13} = 3.393, p = .005; one-sample t test). Three groups of mice exhibited comparable exploration time in the acquisition trials of these tests (Figure S2b,c). In the Y-maze spontaneous alternation task which evaluates spatial working memory, with comparable numbers of entries (Figure S2d), both N3_KD and N1_KD mice showed a noticeable reduction in spontaneous alternation ratios ($F_{2,39}$ = 3.625, p = .036; one-way ANOVA; CT vs. N1_KD: p = .057; CT vs. N3_KD: p = .071; Tukey's post hoc test, Figure 2c), which however did not approach statistical significance.

Taken together, these data indicate that postnatal downregulation of nectin expression, especially nectin-3, in the hippocampus impairs

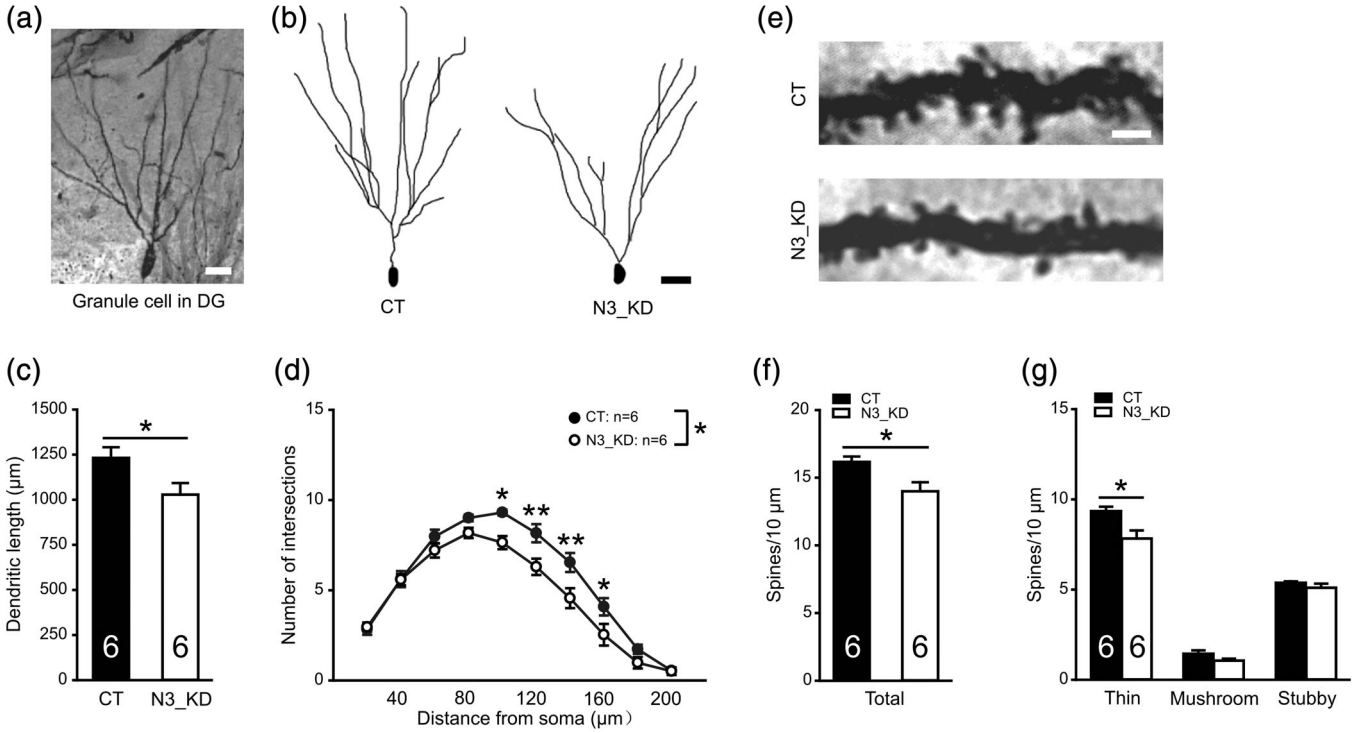

FIGURE 4 Effects of postnatal nectin-3 knockdown on the morphology of DG granule cells in adult dorsal hippocampus. (a) Representative photomicrographs of DG granule cells. Scale bar = 20 μm. (b) Representative dendrite tracings of DG granule cells. Scale bar = 25 μm. (c, d) Total length and complexity of dendrites were reduced in adult mice with postnatal nectin-3 knockdown. (e) Photomicrographs of dendritic segments in DG granule cells. Scale bar = 2 μm. (f, g) The number of dendritic spines, especially thin spines, was reduced in adult mice with postnatal nectin-3 knockdown. *p < .05, **p < .01, compared with the control group. CT, control; DG, dentate gyrus; N3_KD, nectin-3 knockdown

hippocampus-dependent memory functions and had a mild effect on short-term spatial working memory in adult mice.

3.3 | Postnatal nectin-3 knockdown reduced dendritic complexity and spine density in hippocampal principal neurons in adult mice

To reveal the long-term consequences of postnatal nectin-3 or nectin-1 downregulation on the morphology of hippocampal principal neurons, we examined the dendritic morphology and spine density in the adult hippocampus. We first measured the number of neuronal nuclei antigen-positive ($NeuN^+$) neurons in three hippocampal subregions (Figure S3) and found comparable neuronal numbers in three groups (CA1: $F_{2,13}$ = 2.739, p = .102; one-way ANOVA; CT vs. N1_KD: p = .405; CT vs. N3_KD: p = .620; Tukey's post hoc test; CA3: $F_{2,13}$ = 2.683, p = .106; one-way ANOVA; CT vs. N1_KD: p = .299; CT vs. N3_KD: p = .793; Tukey's post hoc test; DG: $F_{2,13}$ = 0.193, p = .827; one-way ANOVA; CT vs. N1_KD: p = .825; CT vs. N3_KD: p = .986; Tukey's post hoc test),

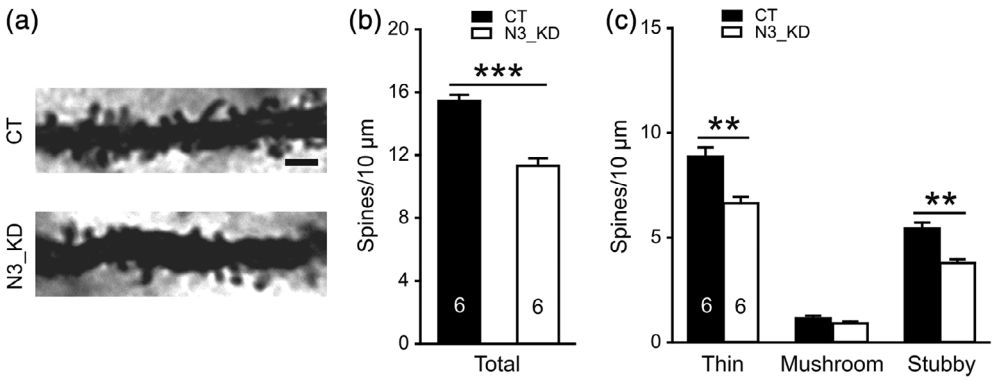

FIGURE 5 Effects of postnatal nectin-3 knockdown on spine density in CA1 pyramidal neurons in adult mice. (a) Photomicrographs of apical dendritic segments of CA1 pyramidal neurons. Scale bar = 2 μm. (b, c) The number of dendritic spines, especially thin and stubby spines, of CA1 pyramidal neurons was reduced by postnatal nectin-3 knockdown. **p < .01, ***p < .001, compared with the control group. CT, control; N3_KD, nectin-3 knockdown

indicating minimal influence of postnatal nectin-3 or nectin-1 knockdown on neuronal loss.

We then quantified the dendritic length and complexity in area CA3 (Figure 3a,b), which is highly vulnerable to early-life stress and abundant with nectin-3. While N1_KD mice had similar dendritic growth compared with the controls, significant reductions were observed in the N3_KD mice in apical dendritic length ($F_{2,15}$ = 5.652, p = .015; one-way ANOVA; CT vs. N1_KD: p = .619; CT vs. N3_KD: p = .014; Tukey's post hoc test) and complexity (main effect of group: $F_{2,15}$ = 5.957, p = .012; group × distance interaction: $F_{40,300}$ = 1.350, p = .086; one-way repeated-measures ANOVA; CT vs. N1_KD: p = 1.000; CT vs. N3_KD: p = .013; Bonferroni post hoc test) (Figure 3c–e). Moreover, reduced spine density was found following postnatal nectin-3 knockdown (Figure 3f,g; $F_{2,15}$ = 13.892, p < .001; one-way ANOVA; CT vs. N1_KD: p = .090; CT vs. N3_KD: p < .001; Tukey's post hoc test). Examination of spine subtypes (Figure 3h) showed that nectin-3 knockdown reduced the density of thin and stubby spines, and nectin-1 knockdown only reduced the density of stubby spines (thin: $F_{2,15}$ = 6.913, p = .007; one-way ANOVA; CT vs. N1_KD: p = .746; CT vs. N3_KD: p = .008; Tukey's post hoc test; mushroom: $F_{2,15}$ = 2.238, p = .141; one-way ANOVA; CT vs. N1_KD: p = .524; CT vs. N3_KD: p = .120; Tukey's post hoc test; stubby:

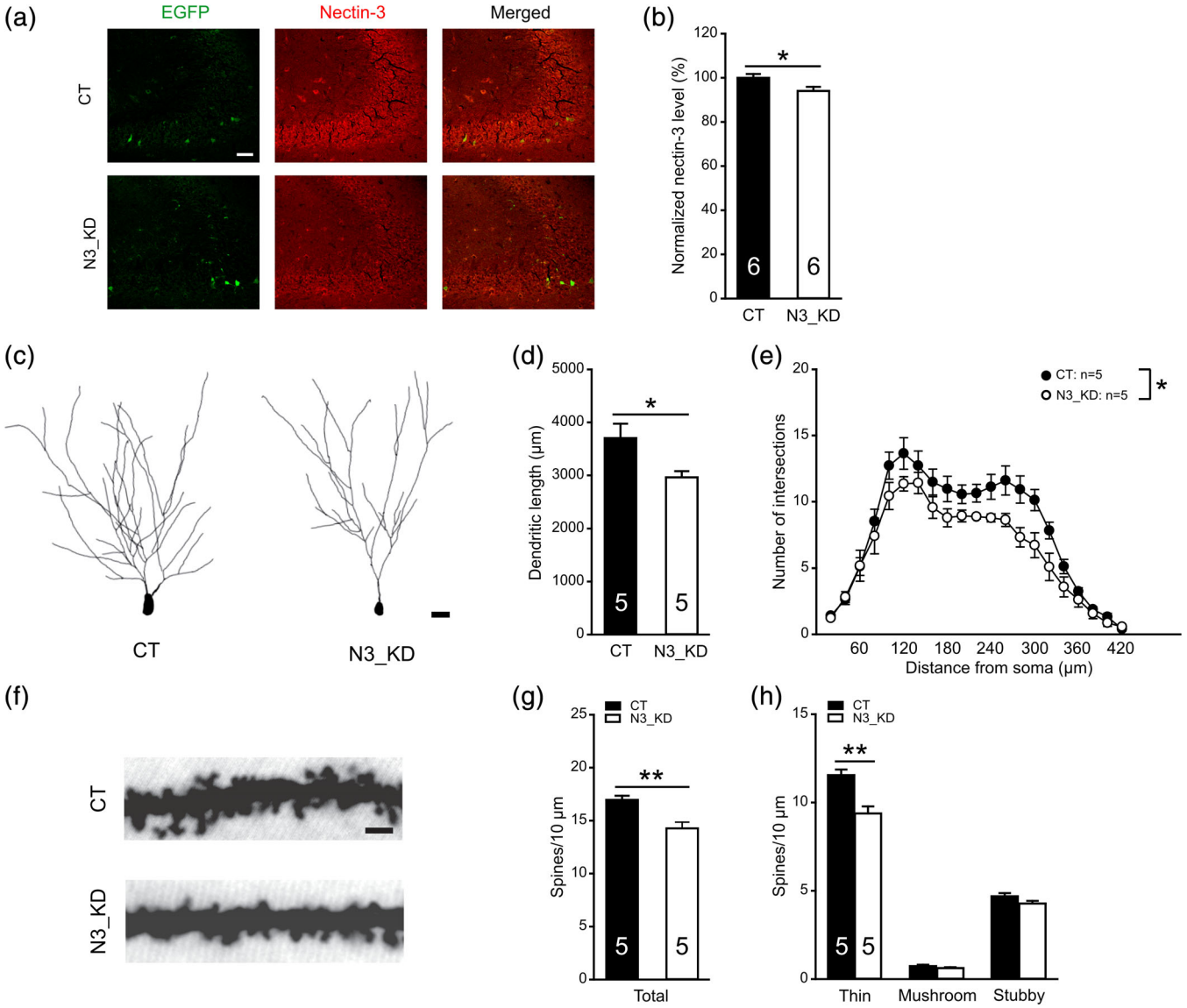

FIGURE 6 Effects of postnatal nectin-3 knockdown on the morphology of the CA3 pyramidal neurons in dorsal hippocampus of infant mice (P16). (a) Images showing EGFP- and/or nectin-3-expressing in the dorsal hippocampus in 16-day-old pups. Scale bar = 50 μm. (b) Postnatal nectin-3 knockdown significantly reduced nectin-3 expression levels in the CA3. (c) Representative tracings of CA3 pyramidal neurons in the two groups. Scale bar = 25 μm. (d, e) Total length and complexity of apical dendrites were reduced in 16-day-old pups with postnatal nectin-3 knockdown. (f) Photomicrographs of apical dendritic segments of CA3 pyramidal neurons. Scale bar = 2 μm. (g, h) The number of dendritic spines, especially thin spines, was reduced by postnatal nectin-3 knockdown in 16-day-old pups. *p < .05, **p < .01, compared with the control group. CT, control; EGFP, enhanced GFP; N3_KD, nectin-3 knockdown

$F_{2,15}$ = 12.326, p = .001; one-way ANOVA; CT vs. N1_KD: p = .010; CT vs. N3_KD: p = .001; Tukey's post hoc test).

Given that mild cognitive and morphological effects were observed in N1_KD mice, for DG and CA1 analysis, we only focused on the effects of nectin-3 knockdown. In DG granule cells (Figure 4a), similar to the effects in CA3, N3_KD mice showed dendritic simplification (length: t_{10} = 2.326, p = .042; unpaired t test; complexity: main effect of group, $F_{1,10}$ = 6.057, p = .034, one-way repeated-measures ANOVA; Figure 4b–d). In terms of dendritic complexity, a significant interaction between group and distance from soma was observed ($F_{9,90}$ = 3.915, p = .0003), which was primarily driven by the reduced number of interactions from 100 to 160 μm in the N3_KD mice (ps < .05; Bonferroni post hoc test). N3_KD mice also exhibited a significant spine loss in the DG granule cells, especially in thin spines (total: t_{10} = 2.777, p = .020; thin: t_{10} = 2.988, p = .014; mushroom: t_{10} = 1.709, p = .118; stubby: t_{10} = 1.098, p = .298; unpaired t test; Figure 4e–g).

We did not analyze dendritic morphology in CA1, because neurons in CA1 were frequently truncated in horizontal sections. For spine density in apical dendrites of CA1 pyramidal neurons, significant reductions were observed in N3_KD mice compared with control ones (total: t_{10} = 6.662, p < .001; thin: t_{10} = 4.106, p = .002; mushroom: t_{10} = 1.510, p = .162; stubby: t_{10} = 4.811, p = .001; unpaired t test; Figure 5).

3.4 | Postnatal nectin-3 knockdown reduced dendritic complexity and spine density in CA3 pyramidal neurons in the infant hippocampus

To examine whether the observed structural abnormalities induced by postnatal nectin-3 knockdown occurred in the early postnatal period, we carried out morphological analyses in 16-day-old pups (2 weeks after viral injection). Some infected neurons in CA3 could already be observed at this early postnatal stage (Figure 6a) and the nectin-3 immunoreactivity was significantly reduced in the N3_KD pups (t_{10} = 2.352, p = .041; Figure 6b).

Compared with control pups, N3_KD showed reduced apical dendritic length (t_8 = 2.512, p = .036; unpaired t test; Figure 6c,d) and complexity (main effect of group: $F_{1,8}$ = 6.338, p = .036; group × distance interaction: $F_{20,160}$ = 1.374, p = .142; one-way repeated-measures ANOVA; Figure 6e). N3_KD mice also exhibited a significant spine loss (total: t_8 = 3.840, p = .005), especially in the thin spines (thin: t_8 = 4.261, p = .003; mushroom: t_8 = 1.176, p = .273; stubby: t_8 = 1.729, p = .122; unpaired t test; Figure 6f–h). These results indicate that postnatal nectin-3 knockdown impairs structural development of the hippocampus in early life.

4 | DISCUSSION

In this study, we downregulated nectin-3 or nectin-1 expression in neonatal mice and investigated the long-term effects on hippocampus dependent cognitive functions and dendritic morphology and spine density in adult hippocampus. We showed that suppression of nectin-3, but not nectin-1, significantly impaired hippocampus-dependent memory and simplified the dendritic structure of principal neurons in the adult hippocampus (P75). We further found that at P16 (2 weeks after viral injection) N3_KD mice also exhibited reduced dendritic length/complexity and spine loss, which suggests that the deleterious effects of postnatal nectin-3 knockdown occur in early life and continue into adulthood. Our findings provide evidence to a fundamental role for nectin-3 on postnatal neurodevelopment of hippocampal structure and function.

Nectins as CAMs locate at the synaptic sites in neuronal axons and dendrites and play an important role in the formation of synapses by altering the spine number and size which is crucial to learning processes (Mizoguchi et al., 2002; Takai et al., 2008; Wang et al., 2017). Abnormal nectin expression has been observed in stressed mice, which may mediate stress-induced impairments in hippocampus-dependent memory and structural plasticity (Liao et al., 2014; van der Kooij et al. 2014; Wang et al., 2013, 2017). In the present study, we directly examined the causal involvement of nectins in hippocampal neurodevelopment. We found that suppression of nectin-3 in hippocampus from early postnatal stage mimicked early-life stress effects, impairing novel object recognition that mainly depends on the neuronal network between hippocampus and perirhinal cortex, and spatial object recognition memory which is specifically regulated by the hippocampus (Cohen et al., 2013; Lupien et al., 2009). In addition, consistent with other findings, short-term spatial working memory evaluated by the Y-maze spontaneous alternation behavior was not significantly altered in mice with nectin-3 knockdown (Wang et al., 2013, 2017). These results suggest that nectin-3 may be partially involved in hippocampus-dependent memory functions.

During brain development, nectin-3 plays essential roles in the establishment of normal hippocampal mossy fiber trajectory, neural growth, and synaptic maturation, dynamically regulating the dendritic structure in hippocampus (Honda et al., 2006; Wang et al., 2013). In line with previous findings, we observed abnormal dendritic growth and distinct spine density reduction in N3_KD mice, which are similar with the effects of early-life stress in hippocampus (Liao et al., 2014; Liu et al., 2016; Turecki et al., 2014; Wang et al., 2013). The deleterious effects of nectin-3 knockdown on dendritic morphology was especially found in thin and stubby spines, suggesting the important role of nectin-3 in dendritic spine plasticity (Bourne & Harris, 2007). Although evidence shows that conventional knockout of nectin-3 from embryonic period disturbs normal axon-dendrite contacts (Honda et al., 2006; Miyata et al., 2017; Okabe et al., 2004), we down-regulated nectin-3 from P2, which is after the formation of main mossy fiber trajectory (Nakahira & Yuasa, 2005), so we did not analyze the effects of nectin-3 knockdown on axon-dendrite contacts. Some studies suggest that nectin-3 may be involved in cell survival through the nectin–afadin complex (Kanzaki et al., 2008; Takai et al., 2008). We did not observe significant alterations of $NeuN^+$ cell number in N3_KD mice, which indicates that cell survival is minimally affected by postnatal nectin-3 knockdown and may not account for the behavioral changes we observed. Together, our data highlight the

importance of nectin-3 in the postnatal development of hippocampal dendritic arbors.

An interesting finding of the current study is that, different from hippocampal nectin-3 knockdown, nectin-1 knockdown had minor effects on spatial working memory and the density of stubby spines in CA3. Adopting the same stress paradigm, we previously reported that early-life stress reduced the expression level of nectin-1 in pups (Liao et al., 2014), while another studies found increased nectin-1 gene expression in postnatally stressed adult mice (van der Kooij, Grosse, Zanoletti, Papilloud, & Sandi, 2015). These findings suggest that unlike nectin-3, nectin-1 may not be persistently down-regulated after stress. In addition, some evidence shows that chronic stress selectively reduced nectin-1 and nectin-3 in different regions (Gong et al., 2018; van der Kooij et al., 2015), suggesting that nectin-1 and nectin-3, which form heterophilic adhesion, may have disparate mechanisms for stress-induced effects. Collectively, these results highlight that, compared with nectin-1, nectin-3 may be the primary molecular target of postnatal stress in hippocampus.

The molecular mechanisms underlying the effects of nectin-3 on dendritic morphology remain unknown. Nectins bind with the adaptor protein, afadin, to form the nectin–afadin complex, which further cooperates with the N-cadherin-catenin complex in the puncta adherentia junctions (PAJs) (Mizoguchi et al., 2002; Tachibana et al., 2000; Togashi et al., 2006). Using the *afadin*-deficient mouse model, studies have shown that afadin deletion disrupts PAJs, reduces spine density, and alters the ultrastructural morphogenesis in the hippocampus (Beaudoin et al., 2012; Majima et al., 2009; Sai et al., 2017). Afadin deletion also induces nectin mislocation in the DG (Majima et al., 2009), without affecting nectin expression levels, suggesting that afadin may serve as a downstream molecule of nectins (Beaudoin et al., 2012). In future studies, it would be interesting to investigate whether afadin is a potential molecular substrate to mediate nectin-3 effects on cognitive and structural measures.

It is worth noting that the present study adopted intracranial AAV injection in neonatal mice (P2) to down regulate nectin expression levels. The viral spreading seemed to be restricted in hippocampus, but it remains possible that other brain regions may be affected as well. Future studies could validate our findings by injecting the AAV directly into the hippocampus or using the hippocampus-Cre-dependent transgenic mice to specifically down regulate nectin levels.

In summary, our study reveals that reduced hippocampal nectin-3 expression from an early postnatal stage impairs the dendritic development of principal neurons in hippocampus, which may in turn contribute to hippocampus-related memory deficits. These findings provide direct evidence to the important role of nectin-3 in early-life development of hippocampal neuronal structure and function.

ACKNOWLEDGMENTS

We thank Prof. Yi Rao (Peking University) for the use of the Neurolucida system. This work was supported by the National Natural Science Foundation of China (grant No. 81571321, 81630031, and 81571312), the National Key Basic Research Program of China (973 program, No. 2015CB856401) and the Beijing Brain Project (grant No. Z171100000117016), the Peking University Medicine Seed Fund for Interdisciplinary Research (BMU2017MX021).

CONFLICT OF INTEREST

All authors reported no biomedical financial interest or potential conflict of interest.

AUTHOR CONTRIBUTIONS

J.L., X.W., and T.S. designed research. R.L., H.W., and H.-L.W. performed research. R.L., J.L., and Y.-A.S. analyzed data. J.L. and R.L. wrote the manuscript.

DATA AVAILABILITY

The data that support the findings of this study are available from the corresponding author upon reasonable request.

ORCID

Ji-Tao Li https://orcid.org/0000-0003-3160-9225

REFERENCES

Alvarez, V. A., & Sabatini, B. L. (2007). Anatomical and physiological plasticity of dendritic spines. *Annual Review of Neuroscience*, *30*, 79–97. https://doi.org/10.1146/annurev.neuro.30.051606.094222

Beaudoin, G. M., 3rd, Schofield, C. M., Nuwal, T., Zang, K., Ullian, E. M., Huang, B., & Reichardt, L. F. (2012). Afadin, a Ras/Rap effector that controls cadherin function, promotes spine and excitatory synapse density in the hippocampus. *The Journal of Neuroscience*, *32*(1), 99–110. https://doi.org/10.1523/JNEUROSCI.4565-11.2012

Bhatt, D. H., Zhang, S., & Gan, W. B. (2009). Dendritic spine dynamics. *Annual Review of Physiology*, *71*, 261–282. https://doi.org/10.1146/annurev.physiol.010908.163140

Bourne, J., & Harris, K. M. (2007). Do thin spines learn to be mushroom spines that remember? *Current Opinion in Neurobiology*, *17*(3), 381–386. https://doi.org/10.1016/j.conb.2007.04.009

Cohen, S. J., Munchow, A. H., Rios, L. M., Zhang, G., Asgeirsdottir, H. N., & Stackman, R. W., Jr. (2013). The rodent hippocampus is essential for nonspatial object memory. *Current Biology*, *23*(17), 1685–1690. https://doi.org/10.1016/j.cub.2013.07.002

Dalva, M. B., McClelland, A. C., & Kayser, M. S. (2007). Cell adhesion molecules: Signalling functions at the synapse. *Nature Reviews. Neuroscience*, *8*(3), 206–220. https://doi.org/10.1038/nrn2075

Fitch, J. M., Juraska, J. M., & Washington, L. W. (1989). The dendritic morphology of pyramidal neurons in the rat hippocampal CA3 area. I. Cell types. *Brain Research*, *479*(1), 105–114.

Forrest, M. P., Parnell, E., & Penzes, P. (2018). Dendritic structural plasticity and neuropsychiatric disease. *Nature Reviews. Neuroscience*, *19*(4), 215–234. https://doi.org/10.1038/nrn.2018.16

Gholizadeh, S., Tharmalingam, S., Macaldaz, M. E., & Hampson, D. R. (2013). Transduction of the central nervous system after intracerebroventricular injection of adeno-associated viral vectors in neonatal and juvenile mice. *Human Gene Therapy Methods*, *24*(4), 205–213. https://doi.org/10.1089/hgtb.2013.076

Glaser, E. M., & Van der Loos, H. (1981). Analysis of thick brain sections by obverse-reverse computer microscopy: application of a new, high clarity Golgi-Nissl stain. *Journal of Neuroscience Methods*, *4*(2), 117–125.

Gong, Q., Su, Y. A., Wu, C., Si, T. M., Deussing, J. M., Schmidt, M. V., & Wang, X. D. (2018). Chronic stress reduces nectin-1 mRNA levels and disrupts dendritic spine plasticity in the adult mouse perirhinal cortex. *Frontiers in Cellular Neuroscience*, *12*, 67. https://doi.org/10.3389/fncel.2018.00067

Griffin, G. D., & Flanagan-Cato, L. M. (2008). Estradiol and progesterone differentially regulate the dendritic arbor of neurons in the hypothalamic ventromedial nucleus of the female rat (*Rattus norvegicus*). *The Journal of Comparative Neurology*, *510*(6), 631–640. https://doi.org/10.1002/cne.21816

Honda, T., Sakisaka, T., Yamada, T., Kumazawa, N., Hoshino, T., Kajita, M., … Takai, Y. (2006). Involvement of nectins in the formation of puncta adherentia junctions and the mossy fiber trajectory in the mouse hippocampus. *Molecular and Cellular Neurosciences*, *31*(2), 315–325. https://doi.org/10.1016/j.mcn.2005.10.002

Jamain, S., Quach, H., Betancur, C., Rastam, M., Colineaux, C., Gillberg, I. C., … Paris Autism Research International Sibpair Study. (2003). Mutations of the X-linked genes encoding neuroligins NLGN3 and NLGN4 are associated with autism. *Nature Genetics*, *34*(1), 27–29. https://doi.org/10.1038/ng1136

Kanzaki, N., Ogita, H., Komura, H., Ozaki, M., Sakamoto, Y., Majima, T., … Takai, Y. (2008). Involvement of the nectin-afadin complex in PDGF-induced cell survival. *Journal of Cell Science*, *121*(Pt 12), 2008–2017. https://doi.org/10.1242/jcs.024620

Kim, J. Y., Ash, R. T., Ceballos-Diaz, C., Levites, Y., Golde, T. E., Smirnakis, S. M., & Jankowsky, J. L. (2013). Viral transduction of the neonatal brain delivers controllable genetic mosaicism for visualising and manipulating neuronal circuits in vivo. *The European Journal of Neuroscience*, *37*(8), 1203–1220. https://doi.org/10.1111/ejn.12126

Kirov, G., Gumus, D., Chen, W., Norton, N., Georgieva, L., Sari, M., … Ullmann, R. (2008). Comparative genome hybridization suggests a role for NRXN1 and APBA2 in schizophrenia. *Human Molecular Genetics*, *17*(3), 458–465. https://doi.org/10.1093/hmg/ddm323

Li, J. T., Xie, X. M., Yu, J. Y., Sun, Y. X., Liao, X. M., Wang, X. X., … Si, T. M. (2017). Suppressed calbindin levels in hippocampal excitatory neurons mediate stress-induced memory loss. *Cell Reports*, *21*(4), 891–900. https://doi.org/10.1016/j.celrep.2017.10.006

Liao, X. M., Yang, X. D., Jia, J., Li, J. T., Xie, X. M., Su, Y. A., … Wang, X. D. (2014). Blockade of corticotropin-releasing hormone receptor 1 attenuates early-life stress-induced synaptic abnormalities in the neonatal hippocampus. *Hippocampus*, *24*(5), 528–540. https://doi.org/10.1002/hipo.22254

Liu, R., Yang, X. D., Liao, X. M., Xie, X. M., Su, Y. A., Li, J. T., … Si, T. M. (2016). Early postnatal stress suppresses the developmental trajectory of hippocampal pyramidal neurons: The role of CRHR1. *Brain Structure & Function*, *221*(9), 4525–4536. https://doi.org/10.1007/s00429-016-1182-4

Lupien, S. J., McEwen, B. S., Gunnar, M. R., & Heim, C. (2009). Effects of stress throughout the lifespan on the brain, behaviour and cognition. *Nature Reviews. Neuroscience*, *10*(6), 434–445. https://doi.org/10.1038/nrn2639

Majima, T., Ogita, H., Yamada, T., Amano, H., Togashi, H., Sakisaka, T., … Takai, Y. (2009). Involvement of afadin in the formation and remodeling of synapses in the hippocampus. *Biochemical and Biophysical Research Communications*, *385*(4), 539–544. https://doi.org/10.1016/j.bbrc.2009.05.097

Miyata, M., Maruo, T., Kaito, A., Wang, S., Yamamoto, H., Fujiwara, T., … Takai, Y. (2017). Roles of afadin in the formation of the cellular architecture of the mouse hippocampus and dentate gyrus. *Molecular and Cellular Neurosciences*, *79*, 34–44. https://doi.org/10.1016/j.mcn.2016.12.007

Mizoguchi, A., Nakanishi, H., Kimura, K., Matsubara, K., Ozaki-Kuroda, K., Katata, T., … Takai, Y. (2002). Nectin: An adhesion molecule involved in formation of synapses. *The Journal of Cell Biology*, *156*(3), 555–565. https://doi.org/10.1083/jcb.200103113

Nakahira, E., & Yuasa, S. (2005). Neuronal generation, migration, and differentiation in the mouse hippocampal primoridium as revealed by enhanced green fluorescent protein gene transfer by means of in utero electroporation. *The Journal of Comparative Neurology*, *483*(3), 329–340. https://doi.org/10.1002/cne.20441

Okabe, N., Shimizu, K., Ozaki-Kuroda, K., Nakanishi, H., Morimoto, K., Takeuchi, M., … Takai, Y. (2004). Contacts between the commissural axons and the floor plate cells are mediated by nectins. *Developmental Biology*, *273*(2), 244–256. https://doi.org/10.1016/j.ydbio.2004.05.034

Ozawa, K., Hashimoto, K., Kishimoto, T., Shimizu, E., Ishikura, H., & Iyo, M. (2006). Immune activation during pregnancy in mice leads to dopaminergic hyperfunction and cognitive impairment in the offspring: A neurodevelopmental animal model of schizophrenia. *Biological Psychiatry*, *59*(6), 546–554. https://doi.org/10.1016/j.biopsych.2005.07.031

Parrish, J. Z., Emoto, K., Kim, M. D., & Jan, Y. N. (2007). Mechanisms that regulate establishment, maintenance, and remodeling of dendritic fields. *Annual Review of Neuroscience*, *30*, 399–423. https://doi.org/10.1146/annurev.neuro.29.051605.112907

Sai, K., Wang, S., Kaito, A., Fujiwara, T., Maruo, T., Itoh, Y., … Mizoguchi, A. (2017). Multiple roles of afadin in the ultrastructural morphogenesis of mouse hippocampal mossy fiber synapses. *The Journal of Comparative Neurology*, *525*(12), 2719–2734. https://doi.org/10.1002/cne.24238

Sandi, C. (2004). Stress, cognitive impairment and cell adhesion molecules. *Nature Reviews. Neuroscience*, *5*(12), 917–930. https://doi.org/10.1038/nrn1555

Shapiro, L., Love, J., & Colman, D. R. (2007). Adhesion molecules in the nervous system: Structural insights into function and diversity. *Annual Review of Neuroscience*, *30*, 451–474. https://doi.org/10.1146/annurev.neuro.29.051605.113034

Spruston, N. (2008). Pyramidal neurons: Dendritic structure and synaptic integration. *Nature Reviews. Neuroscience*, *9*(3), 206–221. https://doi.org/10.1038/nrn2286

Tachibana, K., Nakanishi, H., Mandai, K., Ozaki, K., Ikeda, W., Yamamoto, Y., … Takai, Y. (2000). Two cell adhesion molecules, nectin and cadherin, interact through their cytoplasmic domain–associated proteins. *The Journal of Cell Biology*, *150*(5), 1161–1176. https://doi.org/10.1083/jcb.150.5.1161

Takai, Y., Miyoshi, J., Ikeda, W., & Ogita, H. (2008). Nectins and nectin-like molecules: Roles in contact inhibition of cell movement and proliferation. *Nature Reviews. Molecular Cell Biology*, *9*(8), 603–615. https://doi.org/10.1038/nrm2457

Thompson, C. L., Pathak, S. D., Jeromin, A., Ng, L. L., MacPherson, C. R., Mortrud, M. T., … Lein, E. S. (2008). Genomic anatomy of the hippocampus. *Neuron*, *60*(6), 1010–1021. https://doi.org/10.1016/j.neuron.2008.12.008

Togashi, H., Miyoshi, J., Honda, T., Sakisaka, T., Takai, Y., & Takeichi, M. (2006). Interneurite affinity is regulated by heterophilic nectin interactions in concert with the cadherin machinery. *The Journal of Cell Biology*, *174*(1), 141–151. https://doi.org/10.1083/jcb.200601089

Turecki, G., Ota, V. K., Belangero, S. I., Jackowski, A., & Kaufman, J. (2014). Early life adversity, genomic plasticity, and psychopathology. *The Lancet Psychiatry*, *1*(6), 461–466. https://doi.org/10.1016/s2215-0366(14)00022-4

van der Kooij, M. A., Fantin, M., Rejmak, E., Grosse, J., Zanoletti, O., Fournier, C., … Sandi, C. (2014). Role for MMP-9 in stress-induced downregulation of nectin-3 in hippocampal CA1 and associated behavioural alterations. *Nature Communications*, *5*, 4995. https://doi.org/10.1038/ncomms5995

van der Kooij, M. A., Grosse, J., Zanoletti, O., Papilloud, A., & Sandi, C. (2015). The effects of stress during early postnatal periods on behavior and hippocampal neuroplasticity markers in adult male mice. *Neuroscience*, *311*, 508–518. https://doi.org/10.1016/j.neuroscience.2015.10.058

Wang, X. D., Su, Y. A., Wagner, K. V., Avrabos, C., Scharf, S. H., Hartmann, J., … Schmidt, M. V. (2013). Nectin-3 links CRHR1 signaling to stress-induced memory deficits and spine loss. *Nature Neuroscience*, *16*(6), 706–713. https://doi.org/10.1038/nn.3395

Wang, X. X., Li, J. T., Xie, X. M., Gu, Y., Si, T. M., Schmidt, M. V., & Wang, X. D. (2017). Nectin-3 modulates the structural plasticity of dentate granule cells and long-term memory. *Translational Psychiatry*, *7*(9), e1228. https://doi.org/10.1038/tp.2017.196

Yan, J., Oliveira, G., Coutinho, A., Yang, C., Feng, J., Katz, C., … Sommer, S. S. (2005). Analysis of the neuroligin 3 and 4 genes in autism and other neuropsychiatric patients. *Molecular Psychiatry*, *10*(4), 329–332. https://doi.org/10.1038/sj.mp.4001629

Yuste, R. (2011). Dendritic spines and distributed circuits. *Neuron*, *71*(5), 772–781. https://doi.org/10.1016/j.neuron.2011.07.024

SUPPORTING INFORMATION

Additional supporting information may be found online in the Supporting Information section at the end of this article.

How to cite this article: Liu R, Wang H, Wang H-L, et al. Postnatal nectin-3 knockdown induces structural abnormalities of hippocampal principal neurons and memory deficits in adult mice. *Hippocampus*. 2019;29:1063–1074. https://doi.org/10.1002/hipo.23098